Craig-Bampton Substructuring for Geometrically Nonlinear Subcomponents

Robert J. Kuether
&
Mathew S. Allen
Department of Engineering Physics
University of Wisconsin
Madison, WI 53706
rkuether@wisc.edu msallen@engr.wisc.edu

ABSTRACT

The efficiency of a modal substructuring method depends on the component modes used to reduce the subcomponent models. Methods such as Craig-Bampton (CB) and Craig-Chang have been used extensively to reduce linear finite element models with thousands or even millions of degrees-of-freedom down to a few tens or hundreds. The greatest advantage to these approaches is that they can obtain acceptable accuracy with a small number of component modes. Currently, these modal substructuring methods only apply to linear substructures. A new reduction method is proposed for geometrically nonlinear finite element models using the fixed-interface and constraint modes (collectively termed CB modes) of the linearized system. The reduced model for this system is written in terms of cubic and quadratic polynomials of the modal coordinates, and the coefficients of the polynomials are determined using a series of static loads/responses. This reduction is a nonlinear extension to the Craig-Bampton model for linear systems, and is readily applied to systems built directly in a commercial FEA package. The nonlinear, reduced modal equations for each subcomponent are then coupled by satisfying compatibility and force equilibrium. The efficiency of this new substructuring approach is demonstrated on an example problem that couples two geometrically nonlinear beams at a shared rotational degree-of-freedom. The nonlinear normal modes of the assembled models are compared with those of a truth model to validate the accuracy of the approach.

Keywords: substructuring, reduced order modeling, geometric nonlinearity, component mode synthesis, internal resonance.

1. Introduction

Component mode synthesis (CMS) is used to create a structural dynamic model of an assembly of reduced order subcomponent models. These low order subcomponents are represented by a small set of component modes, significantly reducing the number of coordinates in the equations of motion. In finite element analysis (FEA), CMS is widely used as a method to assemble large scale models that are far too computationally expensive to model in their entirety, for example when the model has millions of degrees-of-freedom (DOF). One of the most popular CMS methods is the Craig-Bampton (CB) approach [1], where the linear equations of motion of a FEA model are reduced using a truncated set of fixed-interface modes, and constraint modes. This method has proven to be effective at significantly reducing the size of the subcomponent models while still producing a very accurate model of the assembly. However, the existing method has only been exploited for linear systems or for linear substructures with nonlinear connections. An extension of the CB method is proposed in this paper for finite element models with geometric nonlinearity by generating a low order set of nonlinear modal equations using the system's linearized fixed-interface and constraint modes.

Engineering structures are typically designed to operate within their linear regime so they can be more easily modeled, but some particular systems may need to operate within their nonlinear range. For instance, concept hypersonic aircraft [2, 3] experience extreme load environments due the high temperatures and pressures associated with high speed flight. The external skin panels of these aircraft are exposed to high pressure loads due to air flow and engine acoustic noise [4], causing the response to have large deformations within the elastic limits of the material. Also, the fluid-structural interaction can produce thermal loads that can potentially cause the

panels to vibrate nonlinearly about a buckled equilibrium state [5, 6]. In order to accurately predict the response of these load-bearing structures, the physical models must account for such phenomena.

Consider the schematic of the air vehicle shown in Fig. 1. The response of a single panel can be computed with an FEA model that accounts for geometric nonlinearity, which are typically on the order of 100,000's of DOF (or higher). However, a model of only a single panel may be insufficient to predict failure since these panels are connected to other adjacent structures (e.g. panels or structural frames) which are not infinitely stiff. A more global model must be analyzed to account for interactions between the panels, which can dramatically change the overall structure's response, but modeling the entire vehicle directly would require millions of physical DOF and when the structure exhibits nonlinearity this is far too computationally expensive for practical analysis. This paper proposes an alternative approach in which a reduced order model (ROM) of each geometrically nonlinear subcomponent is constructed and then the subcomponents are assembled to build a mathematical model of the global structure. This method is unique in that it is specifically designed for systems where the nonlinearities are geometric and hence distributed throughout all of the elements of the FEA model.

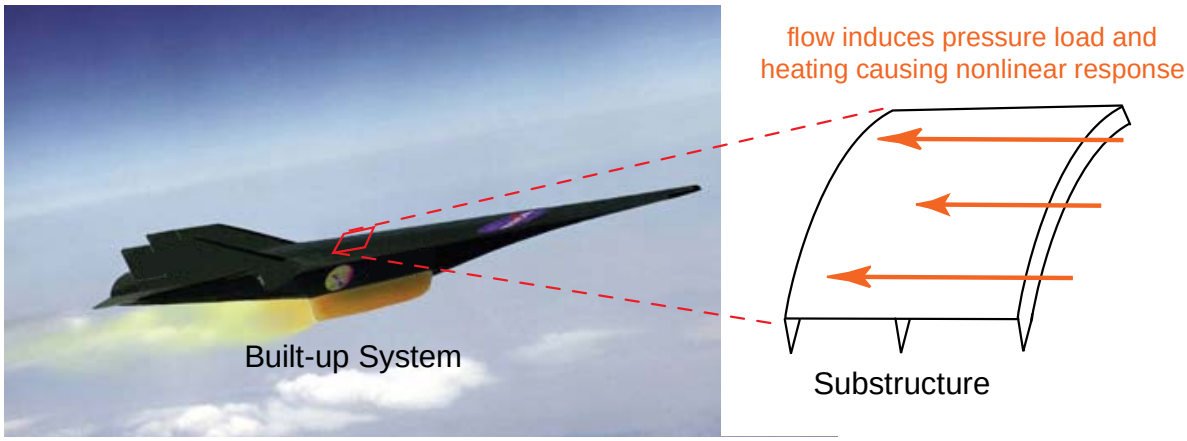

Figure 1. Artists rendition of a concept hypersonic vehicle highlighting a single structural panel.

A number of methods exist to build a reduced order model of a geometrically nonlinear finite element model, as highlighted in [7, 8]. The class of techniques that are of interest here, referred to as *indirect methods*, do not require that the equations of motion be known in closed form, meaning that a ROM can be generated for a nonlinear system built directly within a commercial FEA package. Using the linear (or linearized) modes of the component, a low order set of nonlinear equations can be formulated in terms of the modal coordinates. These modal equations have a diagonal form for the linear modal mass and stiffness matrices, and are augmented with a set of nonlinear coupling terms to account for the geometric nonlinearity. These nonlinear coupling terms are assumed to be well approximated as quadratic and cubic polynomial functions of the generalized coordinates. The polynomial coefficients, which describe the nonlinear stiffness of the structure, are determined by applying a series of static load cases to the structure, computing the nonlinear static response and then using least squares to determine the coefficients that best capture the response. Because these nonlinear reduced order models (NLROMs) typically only require tens of degrees of freedom, they can be used to predict the free or forced response of the system at a dramatically lower cost compared to the direct integration of the full order model.

Most prior applications of NLROMs have been for the response prediction of a geometrically nonlinear component to various inputs (see, e.g. [4, 9, 10]). These works have all use the linearized modes of the system to define the kinematics of the nonlinear equations of motion. While these modes provide an excellent basis to capture the response of a single nonlinear component, they do not provide an optimal basis for substructuring. When this approach is used to derive a ROM for a subcomponent, the result is a substructure model in terms of free-interface modes. However, for linear systems, ROMs with the free-interface modes have long been known to provide a poor basis for a substructure when it will be rigidly attached to another subcomponent; in contrast, the Craig-Bampton method has proven to be very effective at modeling assemblies of linear subcomponents which are joined through stiff connections. This paper extends the CB method to nonlinear subcomponents by formulating a NLROM using the fixed-interface and constraint modes as generalized coordinates. Several of these

NLROMs can then be assembled by satisfying the compatibility and force equilibrium conditions at the interface, as described in [11, 12]. Recently, the authors developed a substructuring approach using NLROMs generated with only free-interface modes [13] (reminiscent of the work in [14]). In the authors' previous work [13], the indirect Implicit Condensation and Expansion [15] method was used to generate the ROM equations of motion from a model built directly in a commercial FEA package. The results showed that many free-interface modes were required in each nonlinear subcomponent to obtain reasonable modal convergence of the assembly. This paper shows that better accuracy can be obtained when using the fixed-interface and constraint modes to build the NLROM.

The paper is outlined as follows. Section 2 introduces the theory behind Craig-Bampton nonlinear reduced order models (CB-NLROMs), and the procedure to couple two or more subcomponents. In Section 3, a case study demonstrates the approach on the coupling of two simply supported beams with geometric nonlinearities. Each subcomponent is reduced to a low order set of equations using the fixed-interface and constraint modes. These models are then coupled, forming a low order set of equations describing the dynamics of the assembly, and the nonlinear normal modes are computed in order to observe the modal convergence of the nonlinear substructuring method. The conclusions are presented in Section 4.

2. Theoretical Development

Starting with the equations of motion for a conservative, N-DOF system discretized by the finite element method,

$$\mathbf{M}\ddot{\mathbf{x}} + \mathbf{K}\mathbf{x} + \mathbf{f}_{NL}(\mathbf{x}) = \mathbf{f}(t) \tag{1}$$

the geometric nonlinearity is defined within the $N \times 1$ nonlinear restoring force vector, $\mathbf{f}_{NL}(\mathbf{x})$, and depends on the strain model used in the large deformation analysis [16, 17]. The $N \times N$ linear mass and stiffness matrices, $\mathbf{M}$ and $\mathbf{K}$, respectively, are generated using linear finite element analysis, and the external loads are defined by the $N \times 1$ vector $\mathbf{f}(t)$.

2.1 Craig-Bampton Nonlinear Reduced Order Model

The physical coordinates, $\mathbf{x}$, capture the displacements and rotations of each node defining the structural model. In order to generate the CB-NLROM of a subcomponent, each coordinate is first partitioned into a set of boundary coordinates, $\mathbf{x}_b$, and interior coordinates, $\mathbf{x}_i$. The boundary coordinates are the DOF that are either shared with an adjacent structure, or have an externally applied load to that location. The interior DOF are the other remaining coordinates that do not experience any loads. The nonlinear equations of motion in Eq. (1) are rearranged as

$$\begin{bmatrix} \mathbf{M}_{ii} & \mathbf{M}_{ib} \\ \mathbf{M}_{bi} & \mathbf{M}_{bb} \end{bmatrix} \begin{Bmatrix} \ddot{\mathbf{x}}_i \\ \ddot{\mathbf{x}}_b \end{Bmatrix} + \begin{bmatrix} \mathbf{K}_{ii} & \mathbf{K}_{ib} \\ \mathbf{K}_{bi} & \mathbf{K}_{bb} \end{bmatrix} \begin{Bmatrix} \mathbf{x}_i \\ \mathbf{x}_b \end{Bmatrix} + \begin{Bmatrix} \mathbf{f}_{NL.i}(\mathbf{x}) \\ \mathbf{f}_{NL.b}(\mathbf{x}) \end{Bmatrix} = \begin{Bmatrix} \mathbf{0} \\ \mathbf{f}(t) \end{Bmatrix} \tag{2}$$

The Craig-Bampton transformation matrix uses two sets of component modes to reduce this partitioned system of equations; namely, the fixed-interface modes and constraint modes [11]. The transformation with these basis vectors is given as,

$$\mathbf{x} = \begin{Bmatrix} \mathbf{x}_i \\ \mathbf{x}_b \end{Bmatrix} = \begin{bmatrix} \mathbf{\Phi}_{ik} & \hat{\mathbf{\Psi}}_{ib} \\ \mathbf{0} & \mathbf{I}_{bb} \end{bmatrix} \begin{Bmatrix} \mathbf{q}_k \\ \mathbf{x}_b \end{Bmatrix} = \mathbf{T}_{CB}\mathbf{q} \tag{3}$$

where $\mathbf{\Phi}_{ik}$ is the $N_i \times N_k$ matrix of mass normalized, fixed-interface modes, $\hat{\mathbf{\Psi}}_{ib}$ is the $N_i \times N_b$ matrix of constraint modes, and $\mathbf{I}$ is the identity matrix. The total number of generalized coordinates in the vector $\mathbf{q}$ is denoted as $m = N_k + N_b$, or the number of fixed-interface modes that have been retained plus the number of boundary coordinates.

The fixed-interface modes are calculated from the linear mass and stiffness matrices for the interior DOF as

$$[\mathbf{K}_{ii} - \omega_j^2 \mathbf{M}_{ii}]\phi_j = \mathbf{0} \qquad j = 1,2,...,N_k \tag{4}$$

and typically only a small number, N_k, of modes must be computed to obtain an adequate model. These fixed-interface modes have zero displacement/rotation at the boundary DOF, and must be augmented with a set of constraint modes to account for deformation at the boundary. The constraint modes are the static deflections that result due to a unit displacement at each boundary coordinate, and are computed from the linear stiffness matrix of the system as

$$\hat{\boldsymbol{\Psi}} = \begin{bmatrix} \hat{\boldsymbol{\Psi}}_{ib} \\ \mathbf{I}_{bb} \end{bmatrix} = \begin{bmatrix} -\mathbf{K}_{ii}^{-1}\mathbf{K}_{ib} \\ \mathbf{I}_{bb} \end{bmatrix} \tag{5}$$

There exist N_b constraint modes, one for each boundary DOF of the subcomponent. The full order model in Eq. (2) is reduced by substituting the CB transformation matrix in Eq. (3), then premultiplying the resulting equation by $\mathbf{T}_{CB}^{\mathrm{T}}$. Then, the CB-NLROM of a single subcomponent is defined by the low order set of equations,

$$\hat{\mathbf{M}}_{CB}\ddot{\mathbf{q}} + \hat{\mathbf{K}}_{CB}\mathbf{q} + \mathbf{T}_{CB}^{\mathrm{T}} \begin{Bmatrix} \mathbf{f}_{NL,i}(\mathbf{q}) \\ \mathbf{f}_{NL,b}(\mathbf{q}) \end{Bmatrix} = \mathbf{T}_{CB}^{\mathrm{T}} \begin{Bmatrix} \mathbf{0} \\ \mathbf{f}(t) \end{Bmatrix} \tag{6}$$

The linear portion is exactly the CB model for a linear subsystem [1, 11]. When the physical model contains geometric nonlinearity, however, additional nonlinear stiffness terms are introduced by $\mathbf{f}_{NL}(\mathbf{q})$. A functional form of the nonlinearity is not readily extracted from models defined directly in commercial FEA packages, so it is difficult to determine this function analytically. Instead, the functional form of the nonlinearity is approximated as

$$\mathbf{T}_{CB}^{\mathrm{T}} \begin{Bmatrix} \mathbf{f}_{NL,i}(\mathbf{q}) \\ \mathbf{f}_{NL,b}(\mathbf{q}) \end{Bmatrix} = \boldsymbol{\theta}(\mathbf{q}) \tag{7}$$

Prior works assume a polynomial function to model the geometric nonlinearity in terms of the free-interface modal coordinates [7, 8], and the same approach is used again here with the CB-NLROM. Hence, the nonlinear function $\boldsymbol{\theta}(\mathbf{q})$ in Eq. (7) is approximated as follows for the r^{th} mode

$$\theta_r(\mathbf{q}) = \sum_{i=1}^{m}\sum_{j=i}^{m} B_r(i,j) q_i q_j + \sum_{i=1}^{m}\sum_{j=i}^{m}\sum_{k=j}^{m} A_r(i,j,k) q_i q_j q_k \tag{8}$$

The nonlinear stiffness coefficients A_r and B_r are then determined using a series of static forces applied to the full order, geometrically nonlinear structure. This is the approach used by the Implicit Condensation and Expansion method in [15] to fit the nonlinear portion of the equations. A static load is applied to the system in Eq. (1), in which the load is in a series of shapes proportional to a combination of the fixed-interface and constraint modes. The multi-modal force is a permutation of the sums and differences of either one, two or three CB modes in the basis set, and is defined as

$$\mathbf{F}_c = \mathbf{M}\left\{\mathbf{T}_{CB,1} f_1 + \mathbf{T}_{CB,2} f_2 + \ldots + \mathbf{T}_{CB,m} f_m\right\} \tag{9}$$

The $N \times 1$ load vector $\mathbf{F}_c$ is a combination of shapes that each have a load scale factor, f_r, for the r^{th} basis vector. The selection of each load factor dictates the level of nonlinearity in each of the characteristic shapes. Typically, each f_r is selected such that the force of a single shape applied to the linear model results in a maximum displacement on the order of the thickness of the structure for low frequency modes, but higher order modes typically require lower displacements [4]. The resulting coefficients tend to be sensitive to the selection of the scaling factor, so in practice a trial and error approach determines which load factors work the best.

Each static load is then applied to the full order model, then the resulting deformation is extracted and the amplitude of each generalized coordinate is computed using the pseudo-inverse of the CB transformation matrix. Using the resulting applied modal forces and displacements, the nonlinear terms A_r and B_r are fit to the reduced static equation,

$$\hat{\mathbf{K}}_{CB}\mathbf{q}+\boldsymbol{\theta}(\mathbf{q})=\mathbf{T}_{CB}^{\mathrm{T}}\mathbf{F}_c \tag{10}$$

The fitting procedure is thoroughly discussed in [4]. After determining the nonlinear static coefficients, the CB-NLROM equations are cast into a matrix form prior to coupling, as done in [18]. First, the quadratic and cubic terms in Eq. (8) are separated into two nonlinear restoring force vectors, $\boldsymbol{\beta}$ and $\boldsymbol{\alpha}$, respectively, as

$$\boldsymbol{\beta}=\begin{bmatrix}\beta_1 & \beta_2 & \dots & \beta_m\end{bmatrix}^{\mathrm{T}} \quad \text{where} \quad \beta_r=\sum_{i=1}^{m}\sum_{j=i}^{m}B_r(i,j)q_iq_j \tag{11}$$

$$\boldsymbol{\alpha}=\begin{bmatrix}\alpha_1 & \alpha_2 & \dots & \alpha_m\end{bmatrix}^{\mathrm{T}} \quad \text{where} \quad \alpha_r=\sum_{i=1}^{m}\sum_{j=i}^{m}\sum_{k=j}^{m}A_r(i,j,k)q_iq_jq_k \tag{12}$$

These vectors are then differentiated with respect to each generalized coordinate in order to produce the quadratic and cubic stiffness matrices as,

$$\mathbf{N}_1(q)=\frac{\partial\boldsymbol{\beta}}{\partial\mathbf{q}}=\begin{bmatrix}\frac{\partial\boldsymbol{\beta}}{\partial q_1} & \frac{\partial\boldsymbol{\beta}}{\partial q_2} & \dots & \frac{\partial\boldsymbol{\beta}}{\partial q_m}\end{bmatrix} \tag{13}$$

$$\mathbf{N}_2(q)=\frac{\partial\boldsymbol{\alpha}}{\partial\mathbf{q}}=\begin{bmatrix}\frac{\partial\boldsymbol{\alpha}}{\partial q_1} & \frac{\partial\boldsymbol{\alpha}}{\partial q_2} & \dots & \frac{\partial\boldsymbol{\alpha}}{\partial q_m}\end{bmatrix} \tag{14}$$

The CB-NLROM in Eq. (6) is then rewritten in matrix form with the nonlinear stiffness matrices in Eqs. (13) and (14) as,

$$\hat{\mathbf{M}}_{CB}\ddot{\mathbf{q}}+\hat{\mathbf{K}}_{CB}\mathbf{q}+\frac{1}{2}\mathbf{N}_1(\mathbf{q})\mathbf{q}+\frac{1}{3}\mathbf{N}_2(\mathbf{q})\mathbf{q}=\mathbf{T}_{CB}^{\mathrm{T}}\begin{Bmatrix}\mathbf{0}\\ \mathbf{f}(t)\end{Bmatrix} \tag{15}$$

A low order CB-NLROM is generated for each subcomponent, and is assembled to adjacent structures using the same approach in [11] for the coupling of linear CB models. The coupling procedure is reviewed for completeness in the following section.

2.2 Coupling with Craig-Bampton Method

Once the CB-NLROMs are generated and in matrix form, the equations are coupled by satisfying both compatibility and force equilibrium at the interface DOF. Consider the assembly of two subcomponents, A and B, whose unconstrained equations of motion are written as

$$\begin{bmatrix}\hat{\mathbf{M}}_{CB}^{A} & \mathbf{0}\\ \mathbf{0} & \hat{\mathbf{M}}_{CB}^{B}\end{bmatrix}\begin{Bmatrix}\ddot{\mathbf{q}}^{A}\\ \ddot{\mathbf{q}}^{B}\end{Bmatrix}+\begin{bmatrix}\hat{\mathbf{K}}_{CB}^{A} & \mathbf{0}\\ \mathbf{0} & \hat{\mathbf{K}}_{CB}^{B}\end{bmatrix}\begin{Bmatrix}\mathbf{q}^{A}\\ \mathbf{q}^{B}\end{Bmatrix}+\frac{1}{2}\begin{bmatrix}\mathbf{N}_1^{A}(\mathbf{q}^{A}) & \mathbf{0}\\ \mathbf{0} & \mathbf{N}_1^{B}(\mathbf{q}^{B})\end{bmatrix}\begin{Bmatrix}\mathbf{q}^{A}\\ \mathbf{q}^{B}\end{Bmatrix}+$$
$$+\frac{1}{3}\begin{bmatrix}\mathbf{N}_2^{A}(\mathbf{q}^{A}) & \mathbf{0}\\ \mathbf{0} & \mathbf{N}_2^{B}(\mathbf{q}^{B})\end{bmatrix}\begin{Bmatrix}\mathbf{q}^{A}\\ \mathbf{q}^{B}\end{Bmatrix}=\begin{matrix}\mathbf{T}_{CB}^{A\,\mathrm{T}}\begin{Bmatrix}\mathbf{0}\\ \mathbf{f}^{A}(t)+\mathbf{r}^{A}(t)\end{Bmatrix}\\ \mathbf{T}_{CB}^{B\,\mathrm{T}}\begin{Bmatrix}\mathbf{0}\\ \mathbf{f}^{B}(t)+\mathbf{r}^{B}(t)\end{Bmatrix}\end{matrix} \tag{16}$$

where $\mathbf{r}(t)$ is the (unknown) reaction force vector applied at each connecting DOF. Compatibility requires that the displacements of the two subcomponents must be equal at the interface, and this leads to a set of constraint equations that can be written as,

$$\mathbf{B}\begin{Bmatrix}\mathbf{x}^{A}\\ \mathbf{x}^{B}\end{Bmatrix}=\mathbf{B}_m\begin{Bmatrix}\mathbf{q}_k^{A}\\ \mathbf{x}_b^{A}\\ \mathbf{q}_k^{B}\\ \mathbf{x}_b^{B}\end{Bmatrix}=\mathbf{0} \tag{17}$$

Equations (16) and (17) are algebraic-differential equations that represent the assembly of two geometrically nonlinear subcomponents. These equations are difficult to solve both analytically and numerically, since any solution to Eq. (16) is constrained by Eq. (17). With the CB models, there is a redundant set of coordinates when two subcomponents are coupled by Eq. (16), since $\mathbf{x}_b^A = \mathbf{x}_b^B$. In order to remove this redundancy from the constrained coordinates, a new set of unconstrained coordinates, $\mathbf{q}_u$, are defined in order to eliminate the need to simultaneously satisfy Eq. (17). The coordinate transformation is defined as,

$$\begin{Bmatrix} \mathbf{q}_k^A \\ \mathbf{x}_b^A \\ \mathbf{q}_k^B \\ \mathbf{x}_b^B \end{Bmatrix} = \begin{bmatrix} \mathbf{I} & \mathbf{0} & \mathbf{0} \\ \mathbf{0} & \mathbf{0} & \mathbf{I} \\ \mathbf{0} & \mathbf{I} & \mathbf{0} \\ \mathbf{0} & \mathbf{0} & \mathbf{I} \end{bmatrix} \begin{Bmatrix} \mathbf{q}_k^A \\ \mathbf{q}_k^B \\ \mathbf{x}_b \end{Bmatrix} = \mathbf{L}\mathbf{q}_u \tag{18}$$

It can be shown that the connectivity matrix, $\mathbf{L}$, lies in the nullspace of the compatibility matrix $\mathbf{B}_m$ in Eq. (17). Therefore, the unconstrained coordinates in Eq. (18) always satisfy the compatibility condition in Eq. (17). This transformation is substituted into Eq. (16), and the resulting equation is premultiplied by $\mathbf{L}^{\mathrm{T}}$. The constrained equation of motion of the assembly becomes

$$\begin{aligned} &\mathbf{L}^{\mathrm{T}} \begin{bmatrix} \hat{\mathbf{M}}_{CB}^A & \mathbf{0} \\ \mathbf{0} & \hat{\mathbf{M}}_{CB}^B \end{bmatrix} \mathbf{L}\ddot{\mathbf{q}}_u + \mathbf{L}^{\mathrm{T}} \begin{bmatrix} \hat{\mathbf{K}}_{CB}^A & \mathbf{0} \\ \mathbf{0} & \hat{\mathbf{K}}_{CB}^B \end{bmatrix} \mathbf{L}\mathbf{q}_u + \frac{1}{2}\mathbf{L}^{\mathrm{T}} \begin{bmatrix} \mathbf{N}_1^A\left(\mathbf{q}^A\right) & \mathbf{0} \\ \mathbf{0} & \mathbf{N}_1^B\left(\mathbf{q}^B\right) \end{bmatrix} \mathbf{L}\mathbf{q}_u + \\ &\qquad + \frac{1}{3}\mathbf{L}^{\mathrm{T}} \begin{bmatrix} \mathbf{N}_2^A\left(\mathbf{q}^A\right) & \mathbf{0} \\ \mathbf{0} & \mathbf{N}_2^B\left(\mathbf{q}^B\right) \end{bmatrix} \mathbf{L}\mathbf{q}_u = \mathbf{L}^{\mathrm{T}} \begin{Bmatrix} \mathbf{T}_{CB}^{A\,\mathrm{T}} \begin{Bmatrix} \mathbf{0} \\ \mathbf{f}^A(t) \end{Bmatrix} \\ \mathbf{T}_{CB}^{B\,\mathrm{T}} \begin{Bmatrix} \mathbf{0} \\ \mathbf{f}^B(t) \end{Bmatrix} \end{Bmatrix} \end{aligned} \tag{19}$$

The differential equations in Eq. (19) completely describe the dynamics of the assembly of subcomponents A and B in terms of the subcomponent CB-NLROMs and the connectivity matrix $\mathbf{L}$. These equations can be integrated to predict the free or forced response of the assembled system of geometrically nonlinear subcomponents. Notice the reaction forces in Eq. (19) are no longer required as they vanish after premultiplying by $\mathbf{L}^{\mathrm{T}}$, as explained in [12, 19]. The modal convergence of the CB-NLROM method will be evaluated in the next section, and compared to the free-interface NLROM substructuring approach developed in [13].

3. Numerical Results

The CB-NLROM nonlinear substructuring approach was explored by coupling two beam models with geometric nonlinearities, using the example presented in [13]. A schematic of this problem is shown in Fig. 2, where the two subcomponent beams were coupled at the appropriate rotational DOF. Each substructure was modeled in Abaqus® using B31 beam elements; the 9-inch beam had a total of 119 DOF, and the 6-inch beam had 89 DOF. The full model of assembly (C) was also constructed in Abaqus® in order to validate the results of the nonlinear substructuring approaches. The subcomponents have the material properties of structural steel with a Young's modulus of 29,700 ksi, shear modulus of 11,600 ksi, and a mass density of $7.36 \cdot 10^{-4}$ lb-s^2/in^4. Both beams had a cross sectional dimension of 0.031 inches thick by 0.5 inches wide.

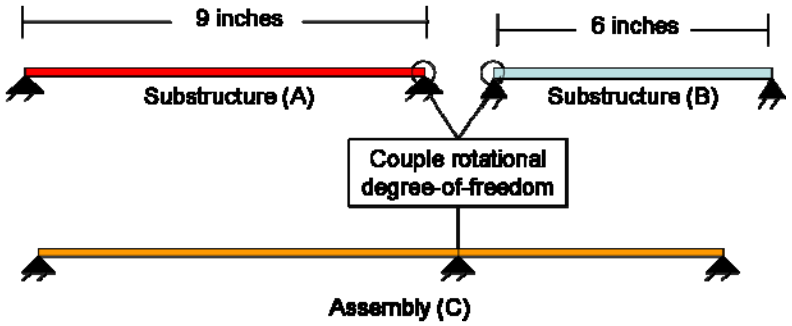

Figure 2. Schematic of coupling of two geometrically nonlinear beams with simply supported boundary conditions.

The interface between each subcomponent had only one DOF, therefore each subcomponent required only a single constraint mode, and a truncated set of fixed-interface modes for the CB-NLROM. In the following, the modal convergence of this approach is compared to the method in [13], where the free-interface modes were used to model each subcomponent. The approach in [13] is termed the NLROM substructuring approach.

3.1 Linear Substructuring Results

First, the linear portion of the 9-inch and 6-inch beam models was used to predict the linear modes of assembly (C) using the free-interface modes approach, and the Craig-Bampton approach, in order to compare their modal convergence for the linear case. To interpret the results, one typically considers the bandwidth of the modes included in each subcomponent model. To facilitate this, the linear natural frequencies for the first eight modes (all bending) of each subcomponent are given in Table 1, along with the exact natural frequencies of the full finite element model of assembly (C) in Fig. 2. The first 5 modes of the assembly are taken to be the modes of interest covering a frequency range from 0 to 500 Hz.

Table 1. Exact linear natural frequencies of finite element models in Fig. 2.

	Simply Support Beam A: 9 inch		**Simply Support Beam B: 6 inch**		**Assembly (C)**
Mode Number	Free-Interface	Fixed-Interface	Free-Interface	Fixed-Interface	Free-Interface
1	34.85 Hz	54.44 Hz	78.41 Hz	122.5 Hz	42.50 Hz
2	139.4 Hz	176.5 Hz	313.8 Hz	397.3 Hz	97.73 Hz
3	313.8 Hz	368.4 Hz	706.4 Hz	829.5 Hz	162.7 Hz
4	558.2 Hz	630.4 Hz	1257 Hz	1420 Hz	313.8 Hz
5	872.7 Hz	962.8 Hz	1966 Hz	2170 Hz	382.1 Hz
6	1258 Hz	1366 Hz	2835 Hz	3080 Hz	588.0 Hz
7	1714 Hz	1840 Hz	3866 Hz	4153 Hz	762.5 Hz
8	2241 Hz	2385 Hz	5059 Hz	5389 Hz	930.0 Hz

A rule of thumb for substructuring with linear subcomponents is to include modes up to 1.5 to 2.0 times the maximum frequency of interest. To be conservative with the target range of 500 Hz, each subcomponent includes modes (either free-interface or fixed-interface) with frequencies up to 1,000 Hz. Then that set of modes was used to predict the modes of the assembly and the errors in each of the predicted natural frequencies are given in Table 2. (The exact frequencies of the FEA assembly are given in the last column of Table 1.) It happens that this frequency range includes the same number of modes, 5 for A and 3 for B, whether fixed-interface or free-interface modes were used.

Table 2. Percent error of predicted linear frequencies of assembly (C) using modes up to 1,000 Hz.

Assembly (C) Mode Number	% Error of Linear Substructuring	
	Free-Interface Modes	CB Modes
1	3.2	$5.5 \cdot 10^{-4}$
2	5.5	$1.6 \cdot 10^{-4}$
3	9.3	$1.9 \cdot 10^{-3}$
4[1]	$2.8 \cdot 10^{-6}$	$2.5 \cdot 10^{-2}$
5	15	$3.4 \cdot 10^{-3}$

Using the free-interface substructuring approach, the maximum frequency error of 15% occurs with the 5th assembly mode. As expected, this modal basis is not well suited for substructuring since the kinematics of the subcomponent do not account for deformation at the interface [11], and one would need far more free-interface modes before the basis could begin to properly describe this motion. In fact, in order to get the frequency error of the free-interface approach below 1% for the first 5 modes of the assembly, each beam needed a total of 72 modes. The CB approach achieves the same performance with each beam having 3 fixed-interface modes, and 1 constraint mode. The CB approach clearly produces a more efficient substructure model because of the kinematics supplied by the constraint modes.

3.2 Validate Nonlinear Reduced Order Models

Next, the NLROMs and CB-NLROMs were generated for each geometrically nonlinear beam in Fig. 2. In the linear case, the CB method needed 5 and 3 modes, respectively, for the 9-inch beam and 6-inch beam in order to predict the assembly modes out to 500 Hz. However, due to the geometric nonlinearity in the models, higher frequency modes can be coupled to lower frequency modes, meaning that more modes are needed in each subcomponent to represent the higher frequency modes of the assembly. Because of this, each subcomponent used a total of 10 modes in the basis.

The NLROMs of each beam included the first 10 linear free-interface modes (all bending) using the ICE approach in [15]. The load scale factors in Eq. (9) were determined such that the amplitude of each force deformed the *linear* structure to a maximum displacement of 0.25 times the beam thickness (or $7.75 \cdot 10^{-3}$ inches). The CB-NLROMs were generated in a similar manner, but instead included the first 10 fixed-interface modes and 1 constraint mode. The load scale factors were chosen such that each force, when applied to the linear structure with no constraints at the interface, produced a maximum displacement of 1.0 times the beam thickness (or 0.031 inches). Both the CB-NLROM and NLROMs were fit using the constrained approach described in [4], in order to preserve the symmetry of the nonlinear stiffness matrices. Both ROMs included the quadratic and cubic polynomials to approximate the nonlinearity, and used static loads that were generated using the reduction factor method (e.g. combinations of forces in the shape of 2 or 3 modes reduced the load factor of each force by a factor of 2 or 3, respectively).

Each subcomponent ROM was validated by computing the first four nonlinear normal modes (NNMs) of the each beam using the pseudo-arclength continuation algorithm in [20]. As discussed in [21], it was suggested that if the NNMs of a ROM converge to the NNMs of the full model, then the ROM will accurately predict the free and forced response of the system. Also, this computation delivered insight into the load scale factors to use when generating the reduced order models. The undamped NNM used in this work is defined as a not-necessarily synchronous periodic response to the conservative, nonlinear equations of motion. A review of NNM theory can be found in [22, 23]. As a reference solution, each NNM of the full order model of the 9-inch and 6-inch beams

[1] Interestingly, because the lengths of the two beams have a ratio 1.5:1, the 4th mode of the assembly is perfectly described by combining one free-interface mode of each, so its natural frequency is estimated very precisely using this basis.

was computed using the Applied Modal Force (AMF) algorithm described in [24]. The NNMs are plotted in Fig. 3a and 3b for the 9-inch and 6-inch beams, respectively, on the frequency versus energy plane. To facilitate this comparison, each NNM frequency was divided by its linearized modal frequency, such that at low energy the branch converges to a frequency value of 1 (or the linear frequency). The energy along the horizontal axis is the total conserved energy of the periodic response.

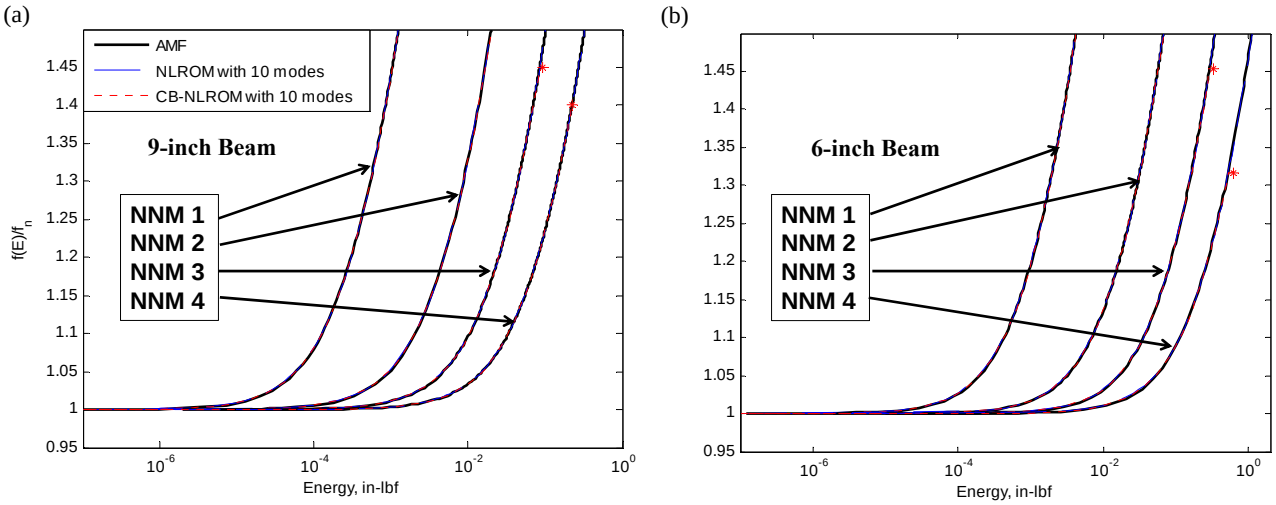

Figure 3. Comparison of the first four NNMs of the (a) 9-inch beam and (b) 6-inch beam using (black) the AMF method on the full FEA model, (blue dashed) a NLROM with 10 free-interface modes, and (red short dashed) a CB-NLROM with 10 fixed-interface modes and 1 constraint mode.

These results show that the NLROM with 10 modes very accurately captured the frequency-energy dependence of the fundamental NNMs of each subcomponent, up to at least a 50% shift in each natural frequency. It is noted that all the NNMs computed with AMF algorithm only required iteration on a single linear (free-interface) bending mode to set the initial condition. This means that no other mode shapes had a significant dynamic contribution to the NNM motion within the range of energy considered for each mode. Since the NLROMs explicitly included modes 1-4 in the basis set, they were also able to accurately compute the frequency-energy dependence of the NNMs.

The CB-NLROMs accurately predicted NNMs 1 and 2 out to a 50% frequency shift for both nonlinear beams, but both models appear to diverge with the third and fourth NNMs. At the solutions marked with an asterisk (*) in Fig. 3, the continuation algorithm began to reduce the step size, and continue along an internal resonance. For example, the third NNM of the 9-inch beam with a CB-NLROM captured a 1:3 internal resonance with the 6th mode of the beam. No internal resonance was computed with the full order model using AMF, suggesting that this was an error introduced by the reduction. However, this was not of primary concern since it was designed to perform well for substructuring, and not representing the free-interface modes of a single component. The CB-NLROMs predict the NNMs of the subcomponents reasonably well, suggesting that the load scale factors were appropriately chosen and the ROM does not have any degenerate behavior.

3.3 Nonlinear Substructuring Results

The nonlinear substructuring methods are now demonstrated on the coupling example in Fig. 2. Once the ROMs were assembled using Eq. (19), the NNMs were computed using the pseudo-arclength continuation algorithm [20]. In Figs. 4 and 5, the first four NNMs of the CB-NLROM and NLROM substructuring approaches are plotted, and compared with those computed by the AMF algorithm on the full order model of the assembly.

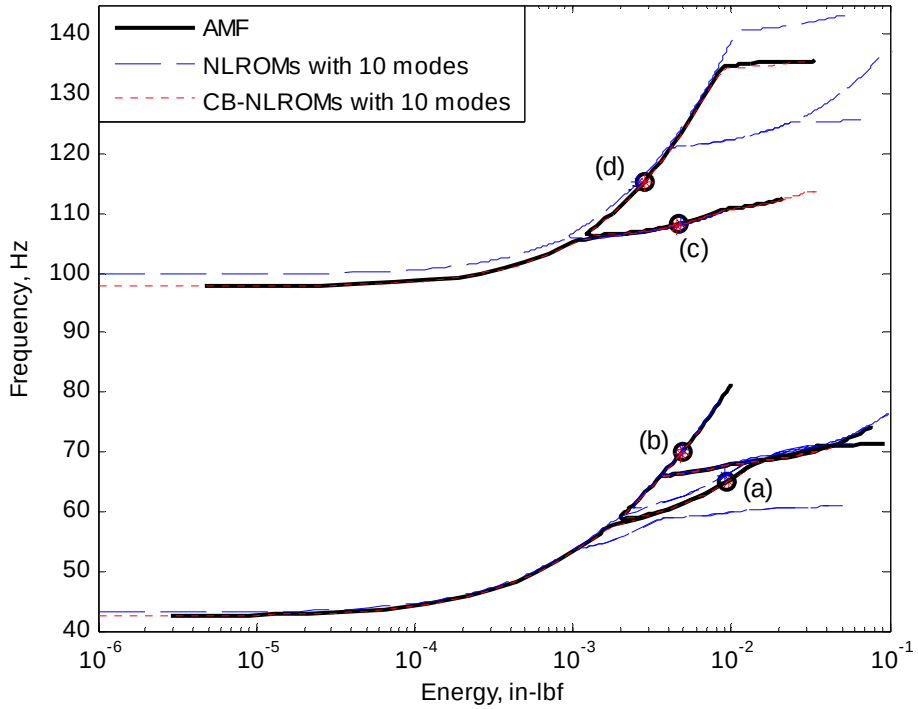

Figure 4. First and second NNMs of the beam assembly using (black) AMF on the full FEA model of the assembly, (blue dashed) two NLROMs with 10 free-interface modes, and (red short dashed) two CB-NLROMs with 10 fixed-interface modes and 1 constraint mode. Time histories and deflection shapes of solutions (a-d) are plotted in Fig. 6.

Each NNM branch initiates at a linear mode at low energy, and continues out to higher response amplitudes as energy increases. At higher energy levels, the geometric nonlinearity was exercised as indicated by the increase in the fundamental frequency. This hardening was caused by the coupling between bending and membrane deformations of the flat structure. As the frequency increased in the NNMs in Figs. 4 and 5, two features were observed in the frequency-energy curves: the backbone and the internal resonances. The backbone traces the solution at the lowest possible energy for a given frequency, and the internal resonances are the tongues that emanate from the backbone. Each internal resonance represents a modal interaction between two or more modes of the structure, with an integer ratio of oscillating frequencies.

The low energy solutions for NNMs 1 and 2 in Fig. 4 show nearly exact agreement between the CB-NLROM approach and the reference solution from AMF, but the NLROM substructuring has some frequency error in this linear range. This error was exactly as predicted by the linear substructuring approach, since the NNMs converge to the linear modes at low energy. As energy increased into the nonlinear region, both the CB-NLROM and NLROM approaches appeared to accurately follow the backbone of the first two NNMs. It should be noted that along the backbone, the NLROM result was always stiffer than the CB-NLROM results, likely due to the fact that more modes would be needed to allow the structure to deform into the correct deflection shape of the coupled system.

The CB-NLROM approach accurately captured the frequencies and energies of the internal resonances observed along NNMs 1 and 2. However, NLROM substructuring predicted only two of these tongues, and introduced new internal resonances. For example, the first tongue along NNM 1 was a 1:3 interaction with NNM 3. The CB-NLROM approach matched the frequencies and energies of this tongue with the AMF results, which initiated around 57 Hz. However, the internal resonance predicted with the NLROM was shifted to a slightly higher frequency, and initiated around 59 Hz. In Fig. 5 one can see that NNM 3 as predicted by the NLROM approach has a frequency error of about 5 Hz at low energy. Since the location of the 1:3 internal resonance with NNM 3 depends on the accuracy of both NNM 1 and NNM 3, the NLROM predicts the wrong frequency for the internal

resonance between these modes. The differences in the features in NNMs 3 and 4, shown in Fig. 5, can be explained in a similar manner. As noted previously, because the beam lengths had a 1.5:1 ratio, the fourth linear mode could be estimated perfectly using two linear modes. Here one also observes that the 4th NNM is also estimated very precisely using the NLROM method. The Craig-Bampton approach also predicts this mode very well, and it does not happen to exhibit internal resonance with any other modes.

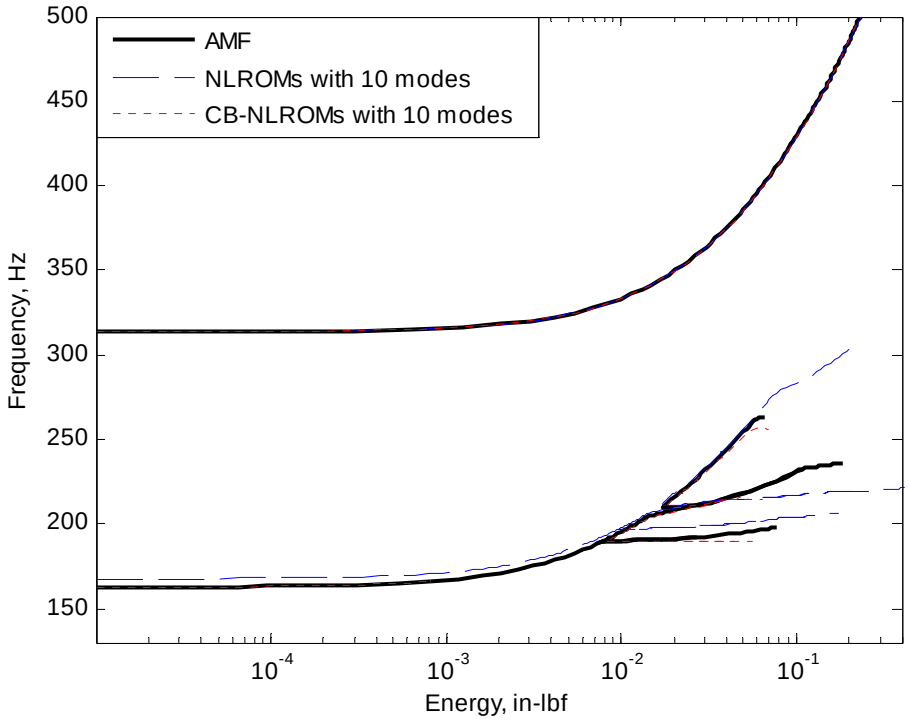

Figure 5. Third and fourth NNMs of the beam assembly using (black) AMF on the full FEA model of the assembly, (blue dashed) two NLROMs with 10 free-interface modes, and (red short dashed) two CB-NLROMs with 10 fixed-interface modes and 1 constraint mode.

The solutions at the points marked (a-d) on NNMs 1 and 2 in Fig. 4 are shown in Fig. 6. The plots in the left column show the maximum deformation (e.g. when all DOF have zero velocity) shape during the periodic response. The time histories in the right column track the transverse displacement of the beam at a location of 4.5 inches from the left end of assembly (C). The deformation shapes computed with the CB-NLROM approach appear to be in very good agreement with the NNMs computed with AMF, except for the solution on the first internal resonance of NNM 1 (Fig. 6a). The deformation shapes computed with the NLROM approach also agree quite well, capturing the shape of the structure with less than 10% error at each point along the two beams. It is interesting to note that these seemingly small errors in capturing the deformation of the structure led to extra internal resonances and completely erroneous branches of NNMs in Figs 4 and 5. The time histories of the periodic responses are also in good agreement between all three methods and once again the CB-NLROM method was noticeably more accurate. Of course, one could have selected regions in the frequency energy plane where the curves would hardly even seem reminiscent. For example, near the spurious 120 Hz internal resonance on the NLROM prediction of NNM 2.

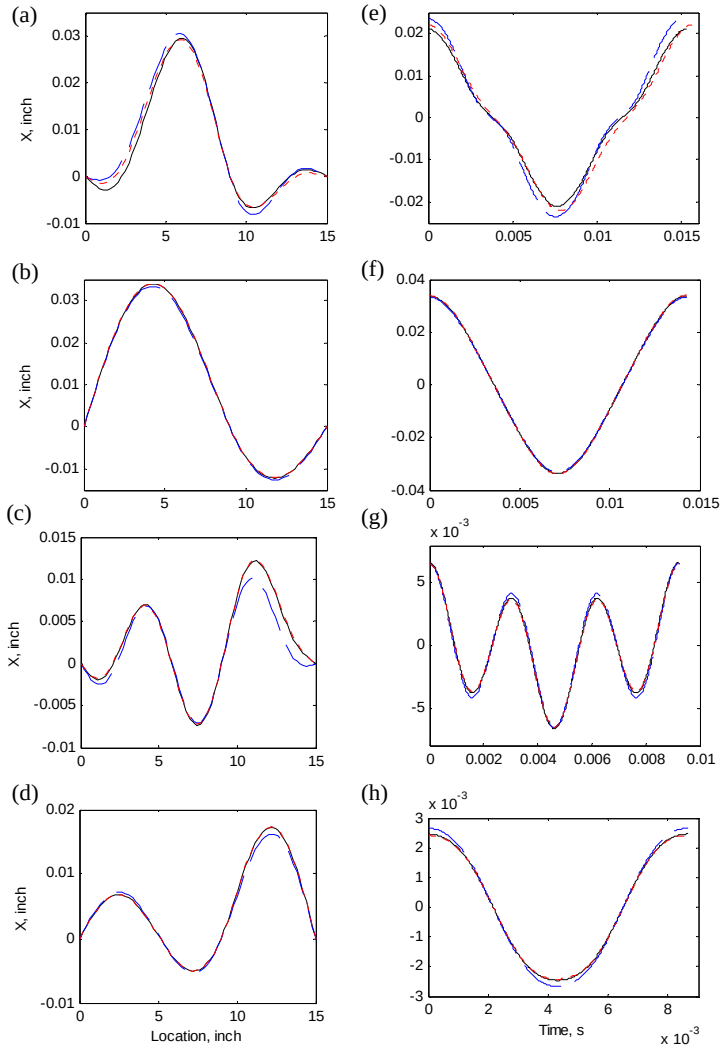

Figure 6. Plots (a-d) are the maximum deformation of the beam assembly corresponding to solutions (a-d) in Fig. 4, respectively, where (black) is AMF, (blue dashed) NLROM substructuring, and (red short dashed) CB-NLROM substructuring. Plots (e-f) show the time history over one period of the transverse displacement of the beam at x = 4.5 inches.

These results show that the CB-NLROM method is capable of producing highly accurate predictions of the NNMs of this assembly, including the internal resonances, so long as enough modes are used to model each subcomponent. Here the CB-NLROM for each subcomponent had a total of 11 basis vectors so after enforcing one constraint the assembly had 21 degrees of freedom. In contrast, the full FEA model, which was used to compute the AMF results, had 207 DOF. On the other hand, the linear substructuring results in Table 2 showed that with only 5 and 3 modes, respectively, of subcomponents A and B, the CB method could predict the first five linear natural frequencies with errors of much less than 1%. The CB-NLROM approach was also used with a smaller number of fixed-interface modes, but in those cases the models seemed to predict spurious internal resonances which made it challenging to compute a large portion of the backbone curve with the continuation algorithm. Hence, those results were not presented here, but this issue will be explored further in subsequent works. On the other hand, perhaps this is to be expected, as nonlinearity couples higher frequency motions to lower ones, so perhaps a reduced order model must be accurate for a much larger frequency band to accurately obtain the first several NNMs.

4. Conclusion

This paper presented a nonlinear modal substructuring approach for geometrically nonlinear finite element models using the Craig-Bampton approach to derive a reduction basis. The fixed-interface modes and constraint modes were generated from the linearized equations of motion and used to estimate a low order set of modal equations to describe the system. The nonlinearity in the modal equations was modeled using quadratic and cubic polynomials and a series of static forces was applied to the full order model to determine the nonlinear stiffness coefficients. The methodology is readily implemented in a commercial finite element package. Once the CB-NLROMs were identified for each subcomponent, the low order equations were coupled at the interface to obtain a mathematical model of the assembly.

The NNMs of the assembled structure showed that CB-NLROM substructuring offered better accuracy than substructuring using free-interface modes, even capturing the true internal resonances of the assembly using only 10 modes of each subcomponent. On the other hand, in the linear case only 5 and 3 modes, respectively, of components A and B were needed to capture the first five modes of the assembly with high accuracy. It is, perhaps, not surprising that quite a few additional modes were needed to accurately model the nonlinear assembly, as nonlinearity can couple low frequency motions to higher frequency motions. The CB-NLROM substructuring presented in this paper used the CB modes as a basis to generate the low order equations of motion, but this approach could be applied to any desired set of basis vectors (for example, free-interface modes with attachment modes as in the Craig-Chang method).

One foreseeable pitfall to the method presented, and indeed to the Craig-Bampton method in general, is the fact that it could require a very large number of constraint modes to capture the kinematics of a continuous interface with many interface DOF. Since one constraint mode is required for each boundary DOF, this could result in a large number of modes in the basis of the NLROM, and several works have shown that the Craig-Bampton basis becomes ineffective when there are many closely spaced boundary nodes (see, e.g. [25]). Furthermore, the computational cost of the NLROM approach grows in proportion to the number of modes in the basis, because many more nonlinear stiffness coefficients must be determined and hence many more static load cases are required [26]. To circumvent this potentially crippling cost, it may be possible to use characteristic constraint modes [27] to reduce the number of constraint modes needed to model a continuous interface.

Acknowledgements

The authors gratefully acknowledge the support of the Air Force Office of Scientific Research under grant number FA9550-11-1-0035, administered by the Dr. David Stargel of the Multi-Scale Structural Mechanics and Prognosis Program.

References

[1] R. R. J. Craig and M. C. C. Bampton, "Coupling of Substructures for Dynamic Analysis," *AIAA Journal*, vol. 6, pp. 1313-1319, 1968.

[2] B. Zuchowski, "Predictive Capability for Hypersonic Structural Response and Life Prediction: Phase II - Detailed Design of Hypersonic Cruise Vehicle Hot-Structure," Air Force Research Laboratory (AFRL), Wright-Patterson Air Force Base, OH AFRL-RQ-WP-TR-2012-0280, 2012.

[3] S. L. Liguore, D. M. Pitt, M. J. Thomas, and N. Gurtowski, "Nonlinear, Low-Order/Reduced-Order Modeling Applications and Demonstration," Air Force Research Laboratory (AFRL), Wright-Patterson Air Force Base, OH AFRL-RB-WP-TR-2011-3102, 2011.

[4] R. W. Gordon and J. J. Hollkamp, "Reduced-Order Models for Acoustic Response Prediction," Air Force Research Laboratory (AFRL), Wright-Patterson Air Force Base, OH AFRL-RB-WP-TR-2011-3040, 2011.

[5] A. J. Culler and J. J. McNamara, "Studies on Fluid-Thermal-Structural Coupling for Aerothermoelasticity in Hypersonic Flow," *AIAA Journal*, vol. 48, pp. 1721-1738, 2010.

[6] A. J. Culler and J. J. McNamara, "Impact of Fluid-Thermal-Structural Coupling on Response Prediction of Hypersonic Skin Panels," *AIAA Journal*, vol. 49, pp. 2393-2406, 2011.

[7] J. J. Hollkamp, R. W. Gordon, and S. M. Spottswood, "Nonlinear modal models for sonic fatigue response prediction: a comparison of methods," *Journal of Sound and Vibration*, vol. 284, pp. 1145-63, 2005.

[8] M. P. Mignolet, A. Przekop, S. A. Rizzi, and S. M. Spottswood, "A review of indirect/non-intrusive reduced order modeling of nonlinear geometric structures," *Journal of Sound and Vibration*, vol. 332, pp. 2437-2460, 2013.

[9] A. A. Muravyov and S. A. Rizzi, "Determination of nonlinear stiffness with application to random vibration of geometrically nonlinear structures," *Computers & Structures*, vol. 81, pp. 1513-1523, 2003.
[10] R. Perez, X. Wang, and M. P. Mignolet, "Nonlinear reduced-order models for thermoelastodynamic response of isotropic and functionally graded panels," *AIAA Journal*, vol. 49, pp. 630-641, 2011.
[11] R. R. J. Craig, *Structural Dynamics*. New York: John Wiley and Sons, 1981.
[12] J. H. Ginsberg, *Mechanical and Structural Vibrations*, First ed. New York: John Wiley and Sons, 2001.
[13] R. J. Kuether and M. S. Allen, "Nonlinear Modal Substructuring of Systems with Geometric Nonlinearities," in *54th AIAA/ASME/ASCE/AHS/ASC Structures, Structural Dynamics, and Materials Conference*, Boston, Massachusetts, 2013.
[14] S. Kawamura, T. Naito, H. M. Zahid, and H. Minamoto, "Analysis of nonlinear steady state vibration of a multi-degree-of-freedom system using component mode synthesis method," *Applied Acoustics*, vol. 69, pp. 624-633, 2008.
[15] J. J. Hollkamp and R. W. Gordon, "Reduced-order models for nonlinear response prediction: Implicit condensation and expansion," *Journal of Sound and Vibration*, vol. 318, pp. 1139-1153, 2008.
[16] M. A. Crisfield, *Nonlinear finite element analysis of solids and structures. Volume 1: Essentials*, 1991.
[17] M. A. Crisfield, *Nonlinear finite element analysis of solids and structures. Volume 2: Advanced Topics*, 1991.
[18] M. Nash, "Nonlinear Structural Dynamics by Finite Element Modal Synthesis," Ph.D, Department of Aeronautics, Imperial College, 1977.
[19] D. de Klerk, D. J. Rixen, and S. N. Voormeeren, "General framework for dynamic substructuring: History, review, and classification of techniques," *AIAA Journal*, vol. 46, pp. 1169-1181, 2008.
[20] M. Peeters, R. Viguié, G. Sérandour, G. Kerschen, and J. C. Golinval, "Nonlinear normal modes, Part II: Toward a practical computation using numerical continuation techniques," *Mechanical Systems and Signal Processing*, vol. 23, pp. 195-216, 2009.
[21] R. J. Kuether, M. R. Brake, and M. S. Allen, "Evaluating Convergence of Reduced Order Models Using Nonlinear Normal Modes," presented at the 32nd International Modal Analysis Conference (IMAC XXXII), Orlando, Florida, 2014.
[22] A. F. Vakakis, "Non-linear normal modes (NNMs) and their applications in vibration theory: an overview," *Mechanical Systems and Signal Processing*, vol. 11, pp. 3-22, 1997.
[23] G. Kerschen, M. Peeters, J. C. Golinval, and A. F. Vakakis, "Nonlinear normal modes. Part I. A useful framework for the structural dynamicist," *Mechanical Systems and Signal Processing*, vol. 23, pp. 170-94, 2009.
[24] R. J. Kuether and M. S. Allen, "A Numerical Approach to Directly Compute Nonlinear Normal Modes of Geometrically Nonlinear Finite Element Models," *Mechanical Systems and Signal Processing*, 2013 (submitted).
[25] P. Blelloch and H. Vold, "Orthogonality and large models – what's the problem? ," presented at the 23rd International Modal Analysis Conference (IMAC XXIII), Orlando, Florida, 2005.
[26] R. Perez, X. Q. Wang, A. Matney, and M. P. Mignolet, "Reduced Order Model For the Geometric Nonlinear Response of Complex Structures," presented at the ASME 2012 International Design Engineering Technical Conferences IDETC/CIE, Chicago, Illinois, 2012.
[27] M. P. Castanier, Y. Tan, and C. Pierre, "Characteristic Constraint Modes for Component Mode Synthesis," *AIAA Journal*, vol. 39, pp. 1182-1187, 2001.